Is Fused Filament Fabrication a Viable Fabrication Method for Bioabsorbable Devices? Development of a 3D Printed Clip for Prevention of Spinal Fusion Infection

A Thesis

Submitted to the Faculty

of

Drexel University

by

Jaclyn Theresia Schachtner

in partial fulfillment of the

requirements for the degree

of

Master of Science in Biomedical Engineering

June 2018

DEDICATION

For my grandmother, Elisabeth Schachtner, at 102 years old you are still the most caring and hardworking person I have had the privilege to know.

ACKNOWLEDGMENTS

This work was supported by the National Institutes of Health (NIAMS) R01 AR069119.

Thank you to Dr. Steven Kurtz, Ph.D. for your guidance and encouragement. I have learned so much these past four years and appreciate all the opportunities the Drexel Implant Research Center afforded me.

To our collaborators at Thomas Jefferson University, thank you for providing vital information, without which this project would not have been possible.

To everyone at the Drexel Implant Research Center, thank you for not just being my coworkers but also my friends. The community you created made coming to work enjoyable even when I was stressed out of my mind. And a special thanks to Christina Arnholt and Hannah Spece, for constantly making themselves available to bounce ideas off and untiringly provide editorial assistance.

Thank you to Dr. Michael Frohbergh, Ph.D. for offering your very limited free time and easing my way into the world of 3D printing, and to all those at Exponent Inc. who worked with me and provided access to machinery I otherwise would not have had the opportunity to use for this project.

Finally, a huge thank you to my parents, sister, and Alexis China. Without your unwavering love and support throughout my years at Drexel, I would not have made it nearly as far as I have.

TABLE OF CONTENTS

LIST OF TABLES

LIST OF FIGURES

LIST OF ABBREVIATIONS

ABS	Acrylonitrile butadiene
ASTM	American Society of Testing and Materials
DSC	Differential scanning calorimetry
EtO	Ethylene oxide
GPC	Gel permeation chromatography
FFF	Fused filament fabrication
PBS	Phosphate buffered solution
PCL	Polycaprolactone
PEO	Polyethylene oxide
PGA	Polyglycolic acid
PLA	Polylactic acid
PLDLLA	Poly-L-co-D,L-lactic acid
PLLA	Poly-L-lactic acid
PVA	Polyvinyl alcohol
SEM	Scanning electron microscope
SLA	Stereolithography (additive manufacturing)

SLS	Selective laser sintering
SSI	Surgical site infection
STL	Stereolithography (CAD file)
TGA	Thermogravimetric analysis
THF	Tetrahydofuran
3D	Three dimensional

ABSTRACT

Lower back pain impacts a majority of the world population at least once in their lifetime. The source of this pain is often due to degenerative changes in the lower spine, sometimes requiring surgical intervention in the form of lumbar spinal fusion. Surgical site infection (SSI) is a serious complication of spinal surgery, affecting as high as 8.5% of the patient population. If the SSI cannot be eradicated with intravenous antibiotic therapy, the next step is a second surgery, involving debridement of the wound and replacing the infected device. Additional surgery not only increases the cost imposed on the patient but also extends recovery time.

In this study, an ultrasound triggered device for the dispersal of antibiotics, was developed as a potential solution. The device is constructed of a bioabsorbable polymer via fused filament fabrication (FFF). This device attaches to a standard 5.5 mm fusion rod and will degrade *in vivo*. Initially, a literature review was performed to determine the most appropriate polymer for this device. Poly-L-co-D,L-lactic acid (PLDLLA) 70/30 was chosen and a filament was fabricated. Gel permeation chromatography (GPC) and differential scanning calorimetry (DSC) analysis were performed to determine the molecular weight and thermal properties of the filament. The filaments were found to be consistent in molecular weight and thermal properties ($p = 0.348$ and $p = 0.487$, respectively). Once analyzed, the filament was then used for FFF printing. Initially, $1cm^3$ cubes were printed for optimization of printing parameters such as print speed and layer height. Then, printing of the spinal clip was attempted. Slight modifications were made to the clip design and printing parameters to reach the final product. Dimensional accuracy was assessed using μCT analysis. There was a difference between the thickness of the

printed clip and the intended design ($p = 0.029$). All other dimensions were found to be similar. To assess the degradation, the clips were incubated at 37°C in PBS for a month and mass loss was measured at one-week time points. Additionally, raw pellets of PLDLLA 70/30 and the filament were degraded, and mass loss was assessed to evaluate how melting the material multiple times impacted the degradation properties. Degradation rate was found to be similar among the samples throughout the first three weeks of degradation however, the raw pellets were found to degrade at a slower rate by the final week ($p = 0.039$).

Further research should focus on additional print optimization as well as determination of the device coating method. Currently, the procedure for device coating involves dipping the device in PLA to create a thin film, but this has proven to result in a coating that is too thick to rupture with ultrasound. The next step would be to formulate a 3D printed coating option to optimize the coating thickness. This study demonstrated a promising future for this device and the viability of not only FFF with PLDLLA but other bioabsorbable polymers, increasing the reach of personalized medicine.

1. INTRODUCTION

1.1 Lumbar Fusion Surgery

Lower back pain is a common problem from which approximately 70% to 85% of the population will suffer during their lifetime [1]. The pain is often localized to the lumbar region, with the risk of its development increasing with age. Lumbar pain can be caused by a multitude of issues, such as trauma, instability, and most commonly, degenerative changes including spondylolisthesis, spondylolysis, disc herniation and degenerative disc disease [2]. Lumbar spinal fusion is used for the treatment of such degenerative diseases and is one of the most common forms of treatment specifically concerning degenerative diseases [3].

Spinal fixation was first developed in the early 1900s by Albee and Hibb, as a response to tuberculosis [4, 5]. Since then, spinal fusion has become increasingly common with roughly 480,000 fusion surgeries performed every year in the United States [4]. The goal of lumbar spinal fusion surgery is to return mechanical integrity to the lumbar spine [2]. The posterolateral fusion technique is currently the gold standard for lumbar fusion surgery as it is minimally invasive, decreasing surgical exposure, operating time, blood loss, and recovery time [6, 7]. Wires, plates, cages, and rod-screw constructs are all used for fusion surgery, however, rod-screw constructs are most commonly use in the lumbar spine (figure 1) [4]. Rod-screw constructs involve inserting pedicle screws bilaterally into the pedicles of vertebrae and joining them with a metal rod, restoring height and stability to the spine [2, 8].

Figure 1: Retrieved implant consisting of three pedicle screws and titanium rod utilized in a spinal fusion. The screws are inserted into the pedicles of the vertebrae and join by the rod, restoring height to the spine segment. The retrieval was provided by the Implant Research Center at Drexel University.

1.2 Surgical Site Infection

Surgical site infection (SSI) is a serious complication of spinal surgery and is reported to affect 1% to 8.5% of individuals after spinal surgery [9-12]. SSIs can develop with any invasive surgery if contamination of the wound site occurs; the severity is dependent on the microorganisms causing the infection [13]. Microorganisms can enter the site via the surgical environment, due to their presence on skin prior to the surgery, from the instruments utilized for the procedure, or from the implanted devices. Additionally, diabetes mellitus, smoking, previous surgery, fusion, extended duration of surgery, and poor general health have been reported to increase the occurrence of SSI [12]. Regardless of the cause, SSIs can have profound consequences such as neurological damage, paralysis, sepsis, and/or death. Specifically, lumbar spine surgeries have reported a 2.1% SSI rate [9]. SSI is indicated by an increase in wound drainage between

10 and 14 days postoperative, increased pain, fever, and reddening of the wound site [9]. A local culture and blood analysis is utilized for the confirmation of a SSI, specifically examining C-reactive protein levels. C-reactive protein is the most responsive to SSI, reportedly increasing in 98% of SSIs [9]. Although medical personnel have strict sanitary guidelines to which they must adhere, there is a need for the creation of additional measures to safeguard against SSIs.

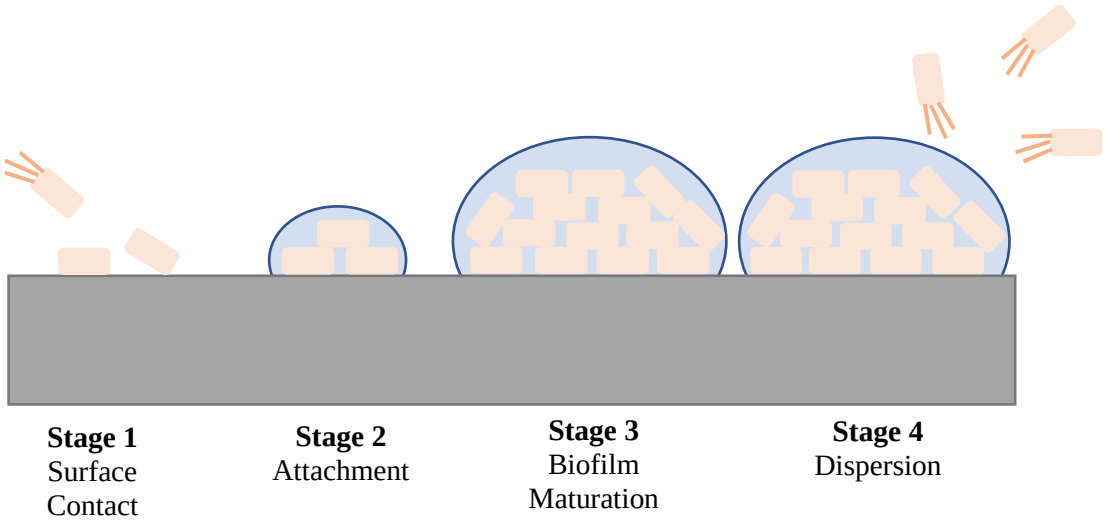

Figure 2: Stages of biofilm development. Bacteria initially make contact with the implantation device. The bacteria adhere to the device and proliferate. The bacteria adhered create a matrix of glycoproteins and use these to securely bind to the implant, affixing the bacteria to the device.

SSIs can be exceedingly hard to destroy due to the development of a biofilm (figure 2). When bacteria populate a wound site and makes contact with the device it creates a matrix of extracellular polysaccharides, also known as a biofilm [14]. The formation the biofilm allows the bacteria irreversibly adhere to the surface of the device essentially making eradication with antibiotics impossible [14]. However, it has been

reported that high levels of vancomycin have shown to cause a steady decline in the concentration of viable bacteria [15].

Treatment of SSIs depends on whether the infection is superficial or deep to the muscular fascia. For more superficial and less serious cases of SSI, intravenous antibiotic therapy is pursued, requiring no further surgery, however, it was reported that this is only utilized in 20% of cases [10]. The remainder of superficial SSI cases required additional surgical debridement [10]. In the case of deep SSI, the wound is debrided, the implant removed, and antibiotics administered. Not only is this a costly procedure, but the patient must then return to the hospital, repeat their rehabilitation process, and at risk of neural injury and deformity progression [10]. It should be noted that prompt treatment of infection yields a 79% success rate [10].

Current methods of treating SSIs in lumbar fusion surgery involve delivering a large dose of systemic antibiotics along with wound debridement. When this approach fails, the surgery is performed again, replacing the contaminated hardware. Between 2001 and 2010, about 3.6 million spinal fusion surgeries were performed in the United States, costing over $287 billion, representing a significant burden on the healthcare system [16].

1.3 Biodegradable Polymers

In the 1980s, environmental issues became more pronounced with accelerating growth of landfills caused by a growing population and culture accustom to discarding items as they pleased [17]. This problem spurred the development of biodegradable polymers in hopes of reducing waste [17]. Although not originally intended for the

biomedical community, biodegradable polymers were of interest. Biodegradable polymers presented the capability to produce a medical device which would degrade once its task was completed. Currently, biodegradable polymers are utilized in numerous biomedical applications, such as drug delivery devices, tissue scaffolds, and sutures [17-22].

While all biodegradable polymers will break down given the correct conditions, they often have vastly different properties. The most important characteristics that determine the behavior of a polymer are the molecular weight and glass transition temperature [17]. Molecular weight of a polymer indicates the weight of one mole of the polymer. Glass transition temperature is the temperature at which the polymer will transition from a glassy state to a rubbery one. The variance in these properties among biodegradable polymers is what dictates the difference in appropriate application of each.

Additionally, there are various categories of materials within the biodegradable family. American Society of Testing and Materials (ASTM) defines biodegradable as "The process of deleterious change in the chemical structure, physical properties, or appearance of a material"[23]. Currently, this definition applies to both bioabsorbable and bioresorbable materials, and ASTM does not address these biodegradable materials separately but singularly by the term *bioresorbable* [24]. Though both materials undergo the defined changes, the byproducts of bioabsorbable material interact with tissue and are metabolized by the body [23, 24]. On the other hand, bioresorbable materials will degrade *in vivo* and the resulting byproducts will be eliminated or absorbed, indicating that the material may or may not interact with cells [24]. This thesis will focus on bioabsorbable materials.

1.4 Three-Dimensional Printing

Three-dimensional (3D) printing was developed in the 1980s by Charles Hull [25]. In efforts to accelerated the production of devices he was developing, he invented stereolithography (SLA) and founded the pioneering company 3D Systems [25, 26]. With the groundwork laid by Hull, Scott Crump of Stratasys developed fused filament fabrication (FFF) in 1990 [27]. FFF functions by heating a thermoplastic material and directly depositing the resulting layers on to a print bed (figure 3)[25]. A spool of filament is placed into the feeding mechanism of the printer and into the nozzle. The material is heated to the appropriate temperature and deposited onto the print bed, building the model layer by layer [28, 29]. In recent years, FFF printing has branched into metal, ceramics, and bioabsorbable polymers [30-33].

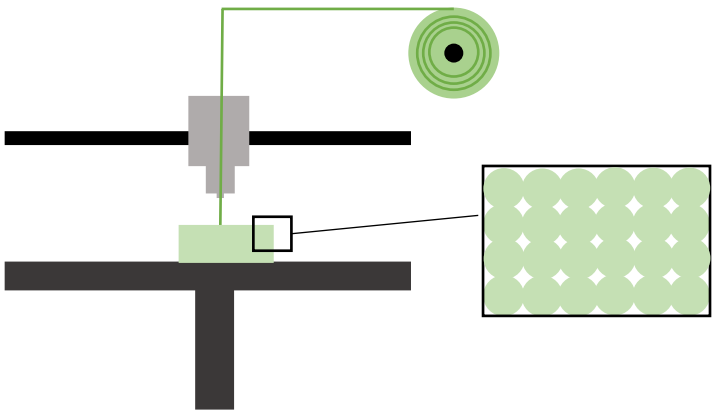

Figure 3: FFF 3D printers deposit semi molten material on to a print bed. The material is fed into to printer from a spool and headed by the nozzle apparatus. The layers of material are laid onto each other, building the print in the z-direction.

3D printers operate with the instruction of a numerical control programming language known as a G-code [34]. Developed by Topcu, Tscioglu and Unver, G-codes present a method for slicing stereolithography (STL) files [35]. G-codes can be created with programs such as Cura, Simplify3D, and Sli3r. Once an STL file is loaded into any of these programs, it is sliced. Slicing begins by finding intersections between triangulated points and identifying the possible cases of intersection (figure 4)[35]. The program will identify the positional relationship between the slicing plane and the facet of interest. After all intersections have been identified, the program then creates lines and groups them, creating a closed loop [35]. Finally, the G-Code is generated by tracing the entire STL file and identifying the start and end points of the print [35].

The G-Code algorithm may vary from program to program and is able to be manipulated by the user. The slicing programs previously mentioned slice the STL file when imported and also provide an interface for the user to customize parameters such as temperature, print speed, object fill, and layer height.

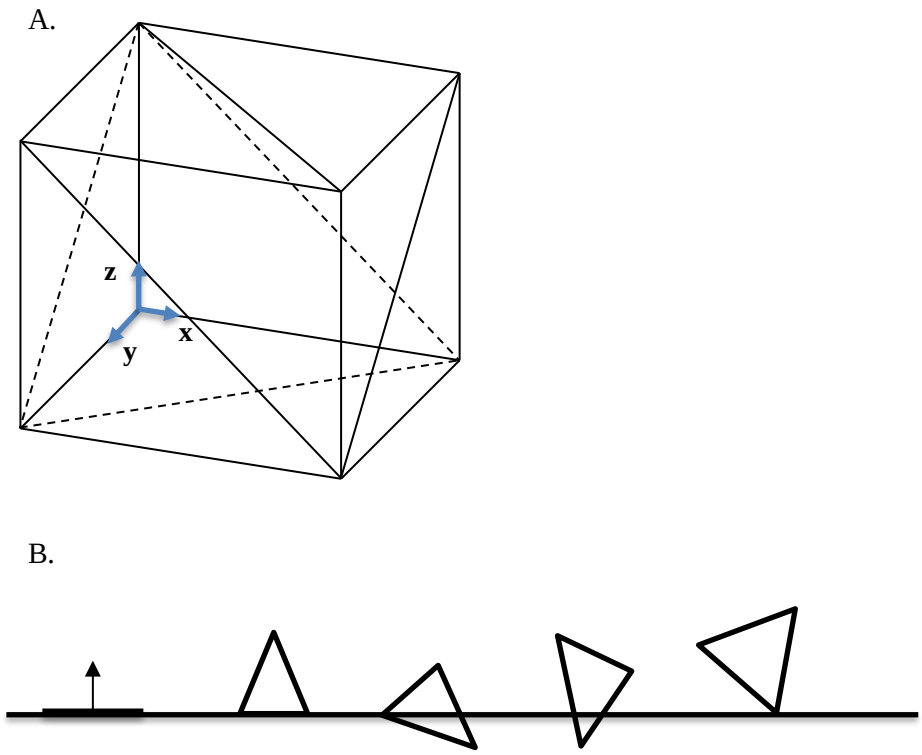

Figure 4: (A) A triangulated cube identifying the twelve facets that would be detected by a slicing program. (B) The five possible cases of intersection [35].

1.5 Study Purpose

SSI has a high rate of occurrence with regards to spinal surgery. Current treatment methods are insufficient as the rate of total implant replacement after infection is high. This poses potential harm to the patients' health as well as significant costs to both the patient and health care system. Bioabsorbable polymers present a potential solution. Creation and application of an implantable drug delivery device will provide a direct release of antibiotics without reopening of the wound, thus decreasing rehabilitation time, cost, and pain the patient is subjected to.

We propose that direct release of antibiotics to the implantation site will aid in the prevention of SSI. The goal of this thesis is to create a hollow device which can be implanted with a rod-screw construct for fusion surgery. This device will be loaded with antibiotics and coated. The device will be ruptured after surgery, providing a burst release of antibiotics without reopening of the surgical site. The device will be constructed of a bioabsorbable polymer, enabling the subsequent degradation of the device.

2. SPECIFIC AIM 1: Selection of Bioabsorbable Polymer

2.1 Aim Description

Bioabsorbable polymers are long-chain molecules composed of repeating units which will dissolve in bodily fluids without cleavage of the polymer chain [22, 36]. Over the past few decades, the use of bioabsorbable polymers in the human body has grown through exploration. Applications of such materials include tissue engineering, orthopedic implants and drug delivery devices [37]. Although their use is increasing, research is still needed to fully understand these materials. Devices constructed of these materials require separate and thorough research into the most appropriate polymer as each device is unique in purpose and goal. For example, rate of degradation is highly variable with chemical structure, mechanical and thermal properties, as well as device design playing a roll [37]. As such, a literature review will be conducted to select the most appropriate bioabsorbable polymer to be used in this application.

The variables of consideration in this review are:

1. Rate of degradation – The material must not degrade prior to day seven of implantation to prevent the premature leaching of antibiotics from the device. The device will be ruptured on day seven or sooner depending on doctor discretion.
2. Biocompatibility – The material must not cause a significant adverse tissue reaction.
3. Ability to 3D print – The material must have glass transition and melting temperatures that can be met by a commercially available FFF printer. The typical

temperature ranges for FFF printer are 15 – 100°C for the print bed and 15 – 300°C for the printing nozzle.

2.2 Polycaprolactone

Polycaprolactone (PCL) has been implemented for multiple devices such as, tissue scaffolds, drug delivery systems, bone, and cartilage applications [21, 38]. PCL is an aliphatic, semi-crystalline polymer composed of cyclic ε-caprolactone and is created through ring-opening polymerization [21, 22, 38, 39]. It has a low melting temperature, reported to be 55 - 65°C and a glass transition temperature of -54°C [22, 38, 39]. PCL breaks down *in vivo* by hydrolytic degradation via surface degradation caused by the cleavage of the polymer backbone on the surface of the polymer [39]. Degradation in this manner will resulting in the device thinning or becoming smaller over time [22]. PCL has been reported to take anywhere from 2 – 4 years to completely degrade depending on the initial molecular weight and configuration of the device [22, 40, 41].

PCL is a widely utilized polymer and, as reported in literature, has an appropriate degradation rate for the application propose here. Additionally, the polymer properties, including degradation rate, can be manipulated by blending it with other materials, such as polyglycolic acid, polylactic acid, and polyethylene oxide (PEO) [21, 22, 42-44]. A possible complication with regards to degradation is the thermal processing the polymer will undergo. The raw polymer is in powder or pellet form. Filament will be created with the raw polymer prior to printing requiring the material to be heated a semi-molten point a minimum of two times. Such processing can decrease the molecular weight resulting in

a lower melting temperature [33]. PCL has a low melting temperature prior to processing; further decrease of temperature has the potential of complicating 3D printing with the material. It has been proven that FFF 3D printing is possible with PCL, however it was achieved by making augmentations to the printer [21]. Moreover, when assessing the printing parameters that should be applied, the print bed should be slightly above the glass transition temperature [45]. The glass transition temperature reported for PCL is -54°C therefore, it cannot be reached by the printer available for this study. Printing could still be possible, however, the print adhesion to the print bed may not be optimal, putting the print resolution at risk. Additionally, a minimal inflammatory response has been observed with PCL [22].

Strengths: • Biocompatible • Previous studies have successfully 3D printed with this material • Degradation rate is appropriate for this application	Weaknesses • Previous 3D printing required modifications to the printer • The print bed will not be able to reach the glass transition temperature without modification or risking print adhesion to the print bed • Risk of minimal inflammatory
Opportunities • PCL has been blended with other bioabsorbable materials for optimal characteristics	Threats • Extensive thermal processing may accelerate degradation rate

Figure 5: SWOT analysis of PCL for the fabrication of a spinal device via FFF printing. PCL is biocompatible and has a degradation rate that is acceptable for this application. The glass transition temperature presents a potential problem for the 3D printing process.

2.3 Polyglycolic Acid (PGA)

Polyglycolic acid (PGA) is an alpha-hydroxyl acid composed of glycolic acid [46]. When stimulated by heat or a catalyst it reacts with another glycolic acid molecules forming the polymer [47]. PGA is biocompatible and degrades in the body by hydrolysis. PGA is currently being used for sutures and other biomedical applications such as tissue scaffolds [48]. Sutures composed of PGA have been reported to have little inflammatory response [47]. However, internal uses of PGA have been reported to illicit a greater response, potentially impacting osteolytic changes [49].

PGA has been reported to have a melting temperature of 224 – 227°C and a glass transition temperature of 35 – 40°C [22, 37]. Both temperatures can be reached by an FFF printer but due to the large difference between the melting and glass transition temperatures, it is possible issues could arise. Standard operation for 3D printing calls for the nozzle to be heated to the melting temperature whereas the printing bed is to be kept at the glass transition temperature. The disparity between the two found here may cause the resolution of the print to be decreased due to inadequate cooling time between layers. The crystallinity of PGA ranges from totally amorphous to a maximum of 52% [37]. When used in a biomedical application PGA is produced with a higher crystallinity to increase the mechanical strength and degradation time. Sutures composed of PGA have been reported to range from 46 – 52% crystallinity. Near or at maximum crystallinity the sutures lose mechanical strength in 2 – 4 weeks and degrade in 90 – 120 days [37, 50]. PGA degradation occurs in a four-stage process. Stage I occurs only a few hours after contact with the solution. The solution diffuses into the polymer and begins the cleavage of the polymer chains through hydrolysis [48]. Similar to PCL, the polymer properties,

including degradation rate, can be manipulated by blending it with other materials, such as PCL, and polylactic acid [44, 51]. It has also been reported that molecular weight decreases when PGA pellets are melted [48]. The pellets will be subjected to melting twice in this application, during filament fabrication and 3D printing. This subjects the polymer to multiple decreases in molecular weight, increasing the already fast degradation rate. Additionally, PGA has been reported to illicit a mild inflammatory response [52].

Strengths: • Biocompatible • Glass transition and melting temperatures are appropriate for the available 3D printer	Weaknesses • The degradation rate is too fast for this application • The range between T_G and T_M is large • Risk of inflammatory reaction
Opportunities • PGA has been blended with other bioabsorbable materials for property optimization	Threats • Extensive thermal processing may accelerate degradation rate

Figure 6: SWOT analysis of PGA for the fabrication of a spinal device via FFF printing. PGL is biocompatible and has glass transition and melting temperatures appropriate for an FFF printer. The rapid degradation rate presents a potential problem as well as a risk of inflammatory reaction.

2.4 Poly-L-lactic Acid (PLLA)

Poly(lactic acid) (PLA) is an alpha-polyester [46, 52]. This material has been utilized in numerous biomedical applications such as, interference screws, sutures, drug

release, and biological membranes [18, 19, 53-55]. PLA has two isomers, the L enantiomer and the D enantiomer (figure 7)[46]. PLA, in the standard filament form provided for FFF 3D printing, is composed of racemic DL-lactide and is amorphous. Poly-levo-lactide (PLLA) is composed of the L-isomer and is semi-crystalline providing different properties to that of standard PLA [36]. PLLA is produced through fermentation carried out by genetically modified strains of microorganisms such as Escherichia Coli [56]. Literature reports the melting and glass transition temperatures as approximately 170 – 180°C and 67 °C, respectively [36, 46, 57]. PLLA degrades by hydrolysis to lactic acid, a compound that is naturally occurring in the body. PLLA may degrade by both surface erosion and bulk erosion [58]. Initially, PLLA will degrade via surface erosion but bulk erosion is highly likely due to the porosity of PLA formulations [59]. Eventually, the lactic acid is broken down further and removed from the body in the form of carbon dioxide and water [60]. The reported degradation rate of PLLA is from 1 – 4 years [36, 52, 61].

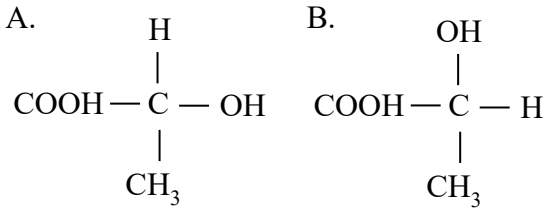

Figure 7: PLA has two optical-stereo isomers. (A) L-lactic acid; (B) D-lactic acid.

PLLA is a biocompatible polymer which has a sufficient degradation rate to remain intact for the necessary time presented by this project. Degradation of PLLA may be slower than necessary due to the high molecular weight and semi-crystallinity of the material however, PLLA has demonstrated the same response to thermal processing as many other materials with the molecular weight decreasing [36]. Holding consistent with the polymers reviewed above, the properties of PLLA, can be manipulated by blending it with other materials, such as PEO, PGA, and PCL [51, 62, 63]. This decrease in molecular weight is likely to result in an accelerated degradation time. Additionally, it has been used as an interbody cage in a goat model. This study showed that the polymer may have a future in spinal applications although there was a mild inflammatory reaction [52].

Strengths: • Biocompatible • Adequate degradation rate • Glass transition and melting temperatures are appropriate for the available 3D printer • Has been used in spinal applications	Weaknesses • Degradation rate is excessively long for this application • Risk of inflammatory reaction
Opportunities • PLLA can be mixed with other materials to optimize properties	Threats • Extensive thermal processing may accelerate degradation rate

Figure 8: SWOT analysis of PLLA for the fabrication of a spinal device via FFF printing. PLLA is biocompatible and has glass transition and melting temperatures appropriate for an FFF printer. The degradation rate is slow for this application and risk of inflammatory reaction presents a potential problem.

2.5 Poly-L-co-D,L-lactic Acid (PLDLLA)

Poly-L-co-DL-lactic acid is composed of poly L-lactide and racemic mix of poly L-lactide and poly D-lactide. The ratio of poly L-lactide to racemic poly-DL-lactide can be augmented based on the application. Ratios that have been used in a clinical application include 80/20, 85/15, and 96/4, while 70/30 is the most common [52]. As the percentage of DL-lactide increases, so will the degradation rate. This is caused by the increase in amorphous D-lactide [36]. PLDLLA 70/30 specifically is composed of 85% L-lactide and 15% D-lactide. Crystallinity and molecular weight are important variables in determining the degradation rate of a polymer [46]. A more highly crystalline polymer will be higher in strength and lower in degradation rate [36]. Crystalline regions will have stronger secondary bonds between polymer chains, resulting in an increased time to degradation as water cannot penetrate easily [36]. By regulating the ratio of L-lactide to the racemic mixture the crystallinity of the polymer is also regulated thus the degradation rate of the polymer can be more highly controlled [55]. The degradation rate of PLDLLA 70/30 has been reported to be 1 – 3 years [55, 64, 65].

PLDLLA 70/30 is a biocompatible polymer which has a sufficient degradation rate for this application. PLDLLA 70/30 has been evaluated for use with spinal cages. These studies have reported no inflammatory response to mild inflammatory response [55]. Should this response be elicited, the opportunity exists to augment the ratio to decrease the degradation rate and reduce the possible build-up of lactic acid. Additionally, the glass transition temperature is appropriate for available FFF printers.

Strengths: • Biocompatible • Glass transition temperature is appropriate for the available 3D printer • Has been used in spinal applications	Weaknesses • Risk of mild inflammatory response
Opportunities • Ratio of the L and DL isomers can be varied for future studies	Threats • Extensive thermal processing may accelerate degradation rate

Figure 9: SWOT analysis of PLDLLA for the fabrication of a spinal device via FFF printing. PLDLLA is biocompatible and has a glass transition appropriate for an FFF printer. The degradation rate is appropriate for this application. Risk of a mild inflammatory reaction presents a potential problem.

2.6 Comparative Matrix

The four polymers identified above all present potential materials for the device proposed here. A matrix was prepared, and the polymers were evaluated on a scale of one (worst) to three (best). The polymers were evaluation based on the three variables of consideration and optimization. Optimization represents the potential for polymer augmentation in future development of the device, i.e. mixing two bioabsorbable polymers for ideal properties.

Table 1: The four polymers discussed were evaluated on a scale from 1 (worst) to 3 (best). The polymers were evaluated on criteria necessary for the successful FFF 3D printing of the device proposed.

Criteria	PCL	PGA	PLLA	PLDLLA
Degradation rate	2	1	2	3
Ability to 3D print	1	2	3	3
Biocompatibility	2	2	2	2
Optimization	2	2	2	3
Total	**7**	**7**	**9**	**11**

2.7 Discussion

While each of the polymers presented here have both strengths and weaknesses concerning this application, 70/30 PLDLLA best fulfills the requirements of this project and poses the least amount of potential risks. PLDLLA has an appropriate degradation and glass transition temperature for 3D printing. Additionally, PLDLLA presents the unique option for augmentation of the ratio of L to DL isomers for heightened control of the degradation rate. There is a risk of mild inflammatory however every polymer reviewed here has been reported to illicit potential inflammatory reaction. PLDLLA was deemed to be the most appropriate polymer for the given application. The polymer was purchased in pellet form (Corbion, Amsterdam, Netherlands).

3. SPECIFIC AIM 2: Filament Creation and Validation

3.1 Aim Description and Hypotheses

Three-dimensional printing has made strides in the past few decades but materials available for printing are limited. The most common materials for FFF printing are acrylonitrile butadiene styrene (ABS) and PLA. Technology is progressing with a greater number of polymers, ceramics and metals available for FFF printing. To date, bioabsorbable polymers remain off this list therefore, prior to printing, filament must be created and validated.

The filament will be created with a single screw extruder (Filabot, Barre, VT) at varying temperatures and speeds for the determination of ideal parameters. To ensure consistent quality of the filament, segments will be taken from different regions of the filament for differential scanning calorimetry and gel permeation chromatography analysis. The hypotheses of this aim are:

1. The filament will show no significant difference in molecular weight or thermal properties at different locations along the filament.
2. The filament will have a lower molecular weight than the raw material due to the filament creation process.

3.2 Requirements and Constraints

The creation and validation of filament must fulfill the following requirements:

1. The filament must measure a diameter between 2.70 – 2.85 mm.
2. The molecular weight of the filament must be consistent.
3. The thermal properties of the filament must be consistent.

The filament is limited to the following constraints:

1. Filament creation must not exceed 1000g of raw material.
2. Costs must not exceed a budget of $3500.

3.3 Temperature Determination

The filament extruder consists of a hopper, mixing chamber, three-stage extrusion screw, and nozzle (figure 10). The hopper holds and heats the material. When the extruder is turned on it feeds into a mixing chamber and eventually the nozzle, from which filament is expelled. The hopper is heated to the desired temperature of the user. Once the temperature is reached, the user may turn on the extruder with the material expelling at a speed chosen by the user.

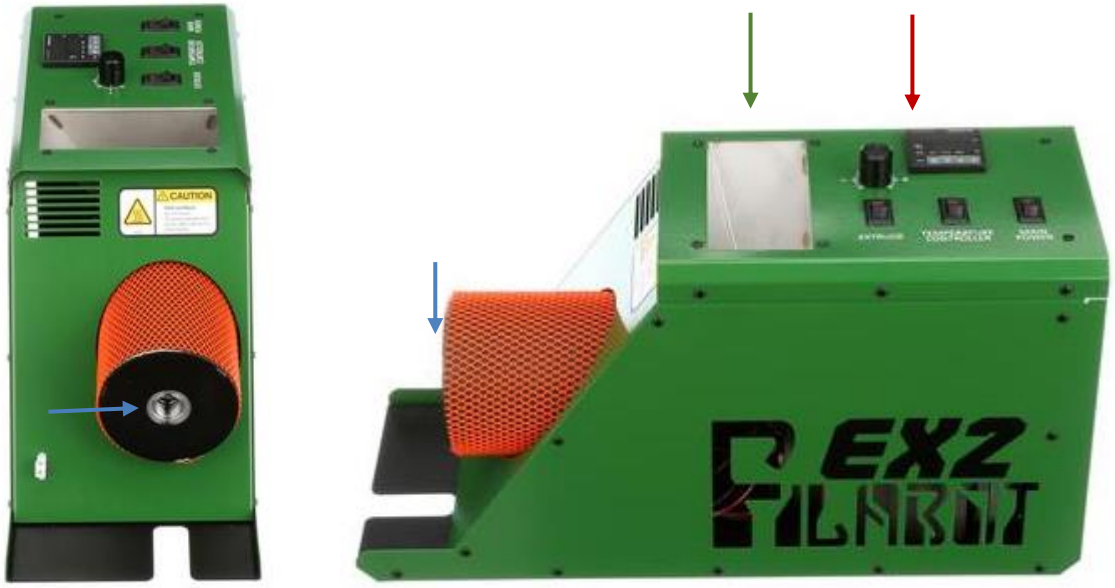

Figure 10: The extruder utilized for filament fabrication. Seen here are the hopper (green arrow), temperature and speed controls (red arrow), as well as the nozzle from which the material is expelled (blue arrow).

PLDLLA (Corbion, Amsterdam, Netherlands) was received in the form of raw pellets. One hundred fifty grams of raw pellets were measured and placed into a Filabot. The Filabot was set to a temperature of 125°C and increased at 5°C increments to a final temperature of 210°C. A small sample was extruded at each temperature. Diameter measurements and observed notes were taken at each temperature. The two samples with the best clarity and consistent diameter were 195°C and 200°C. Once this determination was made the Filabot was cooled, fed with approximately 50 grams of raw pellets and set to 195°C. The temperature was increased at 1°C increments to a final temperature of 200°C. The sample with the best clarity and consistent diameter was produce at 200°C

(mean diameter = 2.81 ± 0.04 mm; figure 11b). With an operating temperature of 200°C, eight filaments, each approximately three feet long were extruded. One sample from the beginning, middle, and end from eight filaments were collected as well as a sample of raw pellet, for a total of 25 samples for analysis.

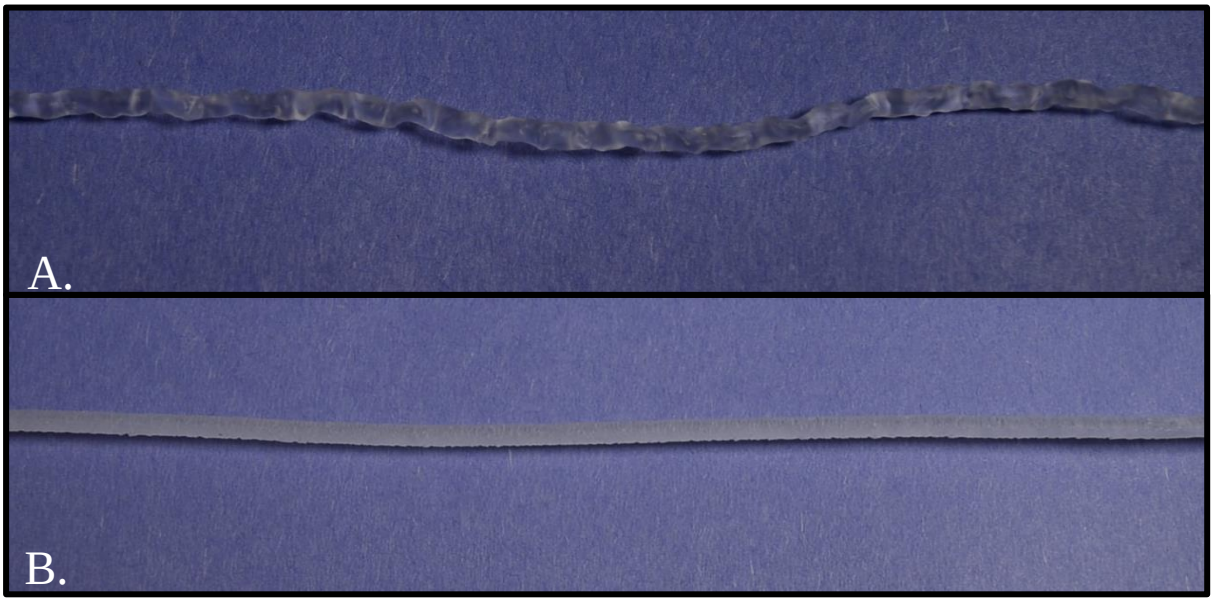

Figure 11: (A) PLDLLA filament produced at a temperature of 170°C. The filament is very irregular in diameter due to temperature as well as extrusion speed. (B) PLDLLA filament produced at a temperature of 200°C. Extrusion at this temperature as well as slow speed produced a filament with a regular diameter.

3.4 Differential Scanning Calorimetry

Differential scanning calorimetry (DSC) is a method used to determine the thermal properties of various materials. DSC operates by measuring the heat absorbed or released as a function of time or temperature [66]. The detection of phase transitions is possible with DSC, by the absorption of heat to the change in temperature [67]. When the

resulting data is plotted as heat flow vs. temperature, the glass transition temperature of amorphous polymers can be determined. This differs from crystalline polymers of which glass transition temperature, crystallization temperature, and melting can be determined. Glass transition temperature signifies the point at which the polymer chains start to release from their coiled position, resulting in the brittleness of the polymer reducing and becoming more ductile [68]. Amorphous polymers never crystallize and, as a result, once these materials exceed the glass transition temperature no defined melting temperature can be identified. Rather, the polymer will show continued heat absorption combined with continual softening.

Prior to DSC analysis, thermogravimetric analysis (TGA) was performed. TGA (TA Instruments, Delaware, USA) was utilized to determine the appropriate temperature range to be used for DSC. TGA measures temperature changes in the material over time, providing information about both physical and chemical properties of the material [8].

DSC (TA Instruments, Delaware, USA) was performed utilizing two pans; one pan was loaded with the material while the other remained empty, as it was used as a reference (figure 12). Both pans were place on top of a heater and heated to 250°C which was inputted into a computer prior to use. The pans were heated at a constant rate of 10°C/min. Requiring the pans to heat at the same rate allows the quantification of additional heat needed for the pan containing the sample to reach the designated temperature when compared to the reference pan. A DSC run was performed on each of the 25 samples of first heating-cooling and second heating. The glass transition temperature was determined from the second heating curve.

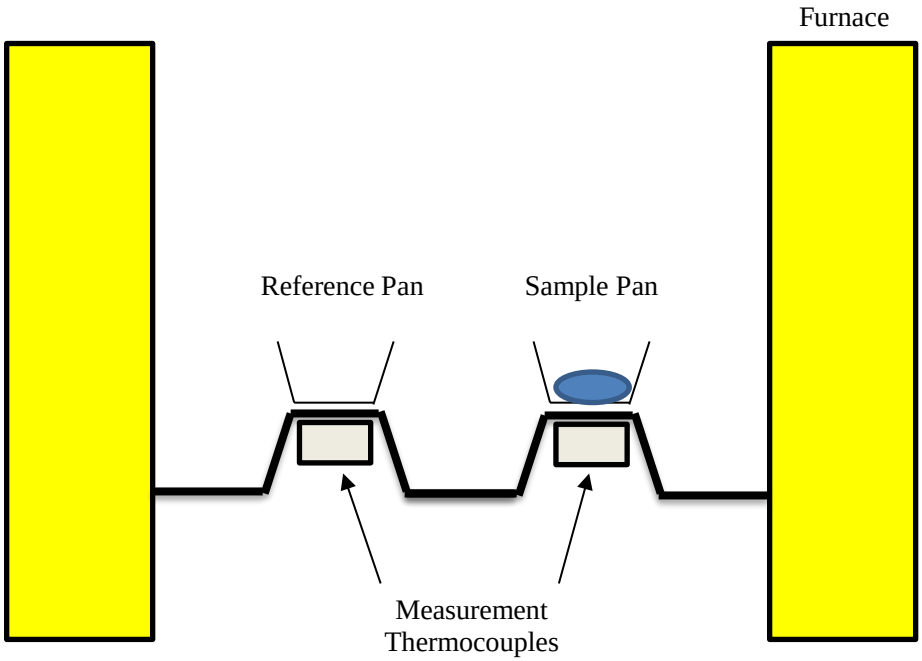

Figure 12: DSC consists of two pans with one used as a reference and the other holding the sample. These pans are heated at the same rate. The different amount of heat required by the pans indicates the heat absorption of the sample

3.5 Gel Permeation Chromatography

Gel permeation chromatography (GPC), specifically size exclusion chromatography, is a method used to determine the molecular weight of a polymer. This technique measures the length of the polymer chains by filtering them based on size. Molecular weight impacts properties such as degradation and mechanical strength. Determining molecular weight of different regions within the filament will determine the uniformity of the filament, providing quality control on the filament production process. Additionally, GPC will provide insight into how thermal processing impacts molecular weight when compared to the raw material.

A GPC apparatus consists of an injection site, a pump, a column, and detector to determine when the sample has left the column. GPC was performed by dissolving each

sample in tetrahydrofuran (THF); dissolution took several days. Once dissolved, the sample was run through a filter and into a GPC column. The filter functions to separate larger chains from traveling further into the column. This process repeats multiple times with the pores continually becoming smaller until eventually exiting the column. One sample was taken from the beginning, middle and end of eight filaments, and one raw sample for a total of 25 samples.

3.6 Results

No difference was found among the samples taken from the created filament, however, only glass transition temperature could be compared ($p = 0.487$; figure 13b). As previously predicted, thermal processing will impact the polymer, figure 13. The thermal properties of the raw pellet differ from those of the fabricated filament. The raw pellet displayed a glass transition temperature and melting temperature (figure 13a). This indicated that prior to the fabrication of the filament the material was semi-crystalline. The lack of recrystallization is likely due to the cooling method of the filament fabrication [69]. The faster the cooling in this step, the more the crystallization will be hindered [69]. This is likely to impact the degradation rate.

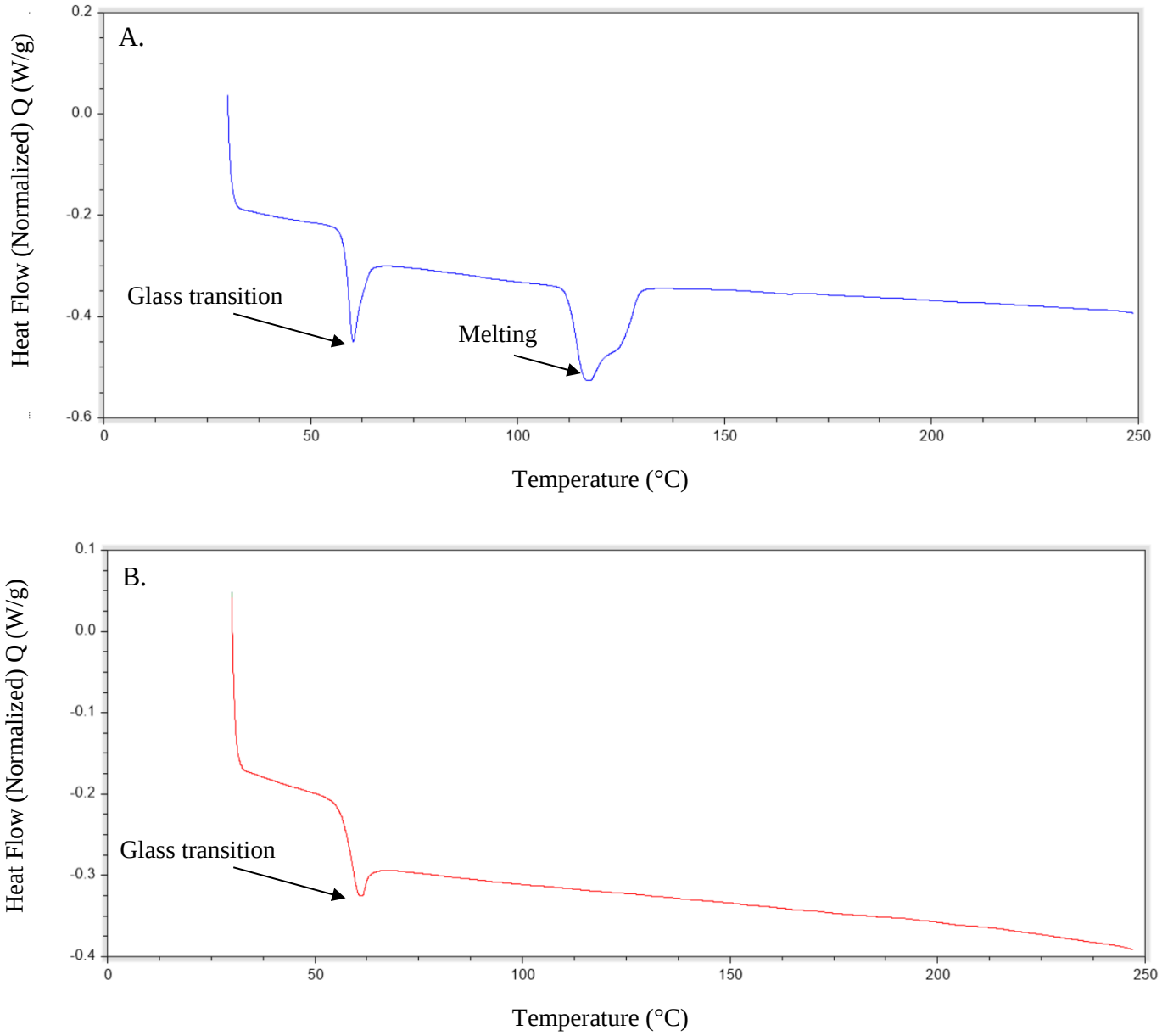

Figure 13: (A) DSC curve of a raw pellet of PLDLLA. The sample displays a glass transition and melting temperature indicating the sample was semi-crystalline. (B) DSC curve of a filament sample of PLDLLA. The sample displays only a glass transition temperature indicating the sample was amorphous.

GPC analysis produced the molecular weight of samples from the beginning, middle and end of filaments, and from one raw sample. All resulting molecular weights from filament samples were found to be similar (ANOVA; $p = 0.348$). Similar to DSC analysis, the GPC analysis of the raw pellet may have different properties than the filament (figure 14). The molecular weight of the raw pellet is higher than that of the filaments however, with a sample size of one this cannot be drawn as a definitive conclusion. A greater sample size is required to confirm if there is a difference.

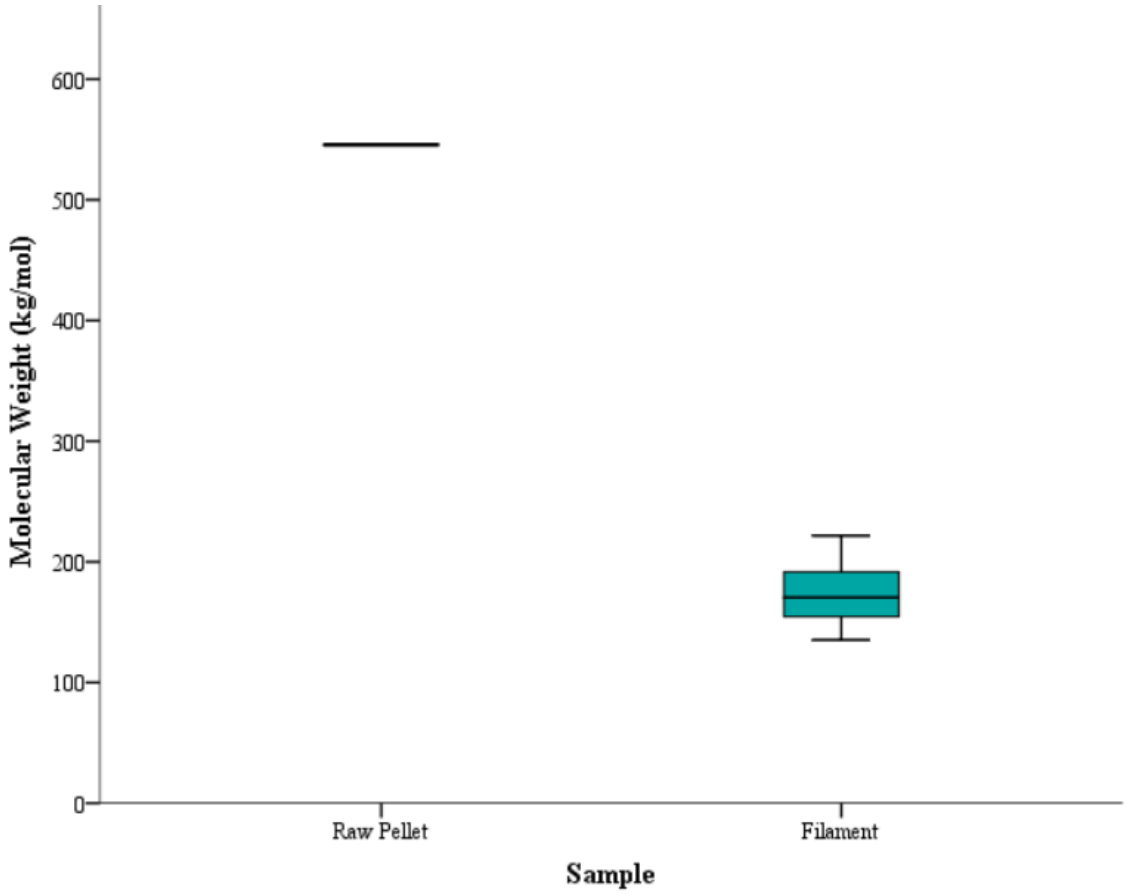

Figure 14: Molecular weight of the raw pellet and filament samples determined with GPC. The molecular weight of the raw pellet may be higher than the filament however the sample size of raw pellet was n = 1 and therefore small to determine significance.

3.7 Discussion

DSC and GPC analysis revealed that the production method of the PLDLLA filament was adequate in producing a filament which held consistent molecular weight and thermal properties throughout. These two variables are significant as they are the governing properties of the degradation rate of the polymer. Additionally, a filament consistent in these properties should also hold when used in 3D printing. However, it should be noted that both the raw sample analyzed for DSC and GPC showed slightly different properties than the filament. Only one sample was analyzed with DSC and GPC and, as such, statistical significance cannot be derived. Still, the raw material appears to have a higher molecular weight and display a melting temperature, whereas the filament only showed a distinct glass transition temperature. This difference is likely due to a slight degradation of the polymer resulting from melting during the filament fabrication process [69].

3.8 Conclusion

PLDLLA 70/30 raw material has the ability to be formed into a filament. The filament was measured to be within the 2.70 – 2.85mm diameter requirement. The filament was found to be consistent in molecular weight and thermal properties throughout however, both the crystallinity and molecular weight of the raw material appeared to be higher than the filament. With a sample size of one raw pellet no statistical difference could be determined to confirm the disparity between raw pellet and filament. The potential difference may have been due to cooling or laboratory conditions.

Further research is required to determine if there is a difference and how it may impact the device.

4. SPECIFIC AIM 3: Clip Fabrication and Degradation

4.1 Aim Description and Hypotheses

Bioabsorbable polymers have been used in clinical applications, such as screws, sutures, and tissue scaffolds. Depending on the polymer, implantation location, and design of the device, degradation rate will vary. To date, no device has been constructed via FFF with a bioabsorbable polymer for the spine. I hypothesize that:

1. The PLDLLA 70/30 filament created can be used for FFF 3D printing.
2. The clip will not have greater than 1% mass loss after a week of *in vitro* degradation.

4.2 Requirements and Constraints

The clip must fulfill the following requirements:

1. The clip must not interfere with the spinal fusion device.
2. The clip must contain an opening for the dispersal of antibiotics.

The clip is limited to the following constraints:

1. The clip must have the ability to be created with a commercially available FFF printer.
2. Optimization of printing parameters must not exceed 500g of trial material.

4.3 Clip Design

The clip was designed to attach to a standard 5.5 mm spinal fusion rod between pedicle screws. As previously determined by Sevit et al., the distance between pedicle screws is 12.00 mm. To insure the clip does not interfere with the spinal rod, the clip height was designed to be 9.00 mm. Two circular channels, 3mm in diameter, were placed 45° off center, for the burst release of antibiotics. The clip is designed to fit as a flush attachment to the spinal fusion rod.

During the production process of the clip, a few slight modifications were made (figure 15). Sharp points are difficult to produce with an FFF printer due to the diameter of the nozzle. Posterior edges of the clip which meet the spinal rod were rounded slightly. Additionally, the superior face of the clip was rounded at the edges. This change was made due to the design of the clip. This clip must be printed without the use of support material as it requires dissolution in water. Rounding the edge provides easier adhesion for the 'lid' of the clip.

Figure 15: Images of the original (left) and modified (right) clip design. The differences include the rounding of the superior edge and rear edges at the location of attachment.

4.4 Clip Manufacturing

The clip was manufactured with FFF 3-dimenional printing (BCN3D Technologies, Barcelona, Spain) and open source software for print optimization (Slic3r). A total of 30 trial prints were completed to determine the optimal printing parameters. The variables of interest were: layer height, number of solid layers, fill pattern, infill speed, travel speed, gap fill speed, and retraction length. Table 2 details the changes that were made during trial printing. The initial printing parameters were the standard parameters used for PLA. Modifications were made until a clip was produced which appeared to have adequate dimensions by visual inspection. The final parameters can be found in the last row of table 2. The resulting clip fit flush to a 5.5mm spinal rod (figure 16).

Table 2: Truncated printing parameters dictating the variables with the greatest number of modifications. The initial parameters are the standard setting for PLA prints. The final row displays the final parameters used for clip production.

Print	Layer Height (mm)	Solid Layers	Fill Pattern	Infill speed (mm/s)	Travel speed (mm/s)	Gap fill speed (mm/s)	Retraction length (mm)
1	0.2	2	Rectilinear	50	130	20	2
2	0.2	2	Concentric	50	130	20	2
3	0.2	2	Honeycomb	50	130	20	2
4	0.2	2	Honeycomb 3D	50	130	20	2
…							
27	0.1	5	Honeycomb 3D	40	80	10	1
28	0.1	5	Honeycomb 3D	60	80	10	1
29	0.1	5	Honeycomb 3D	50	80	10	1
30	0.1	5	Honeycomb 3D	50	80	10	1

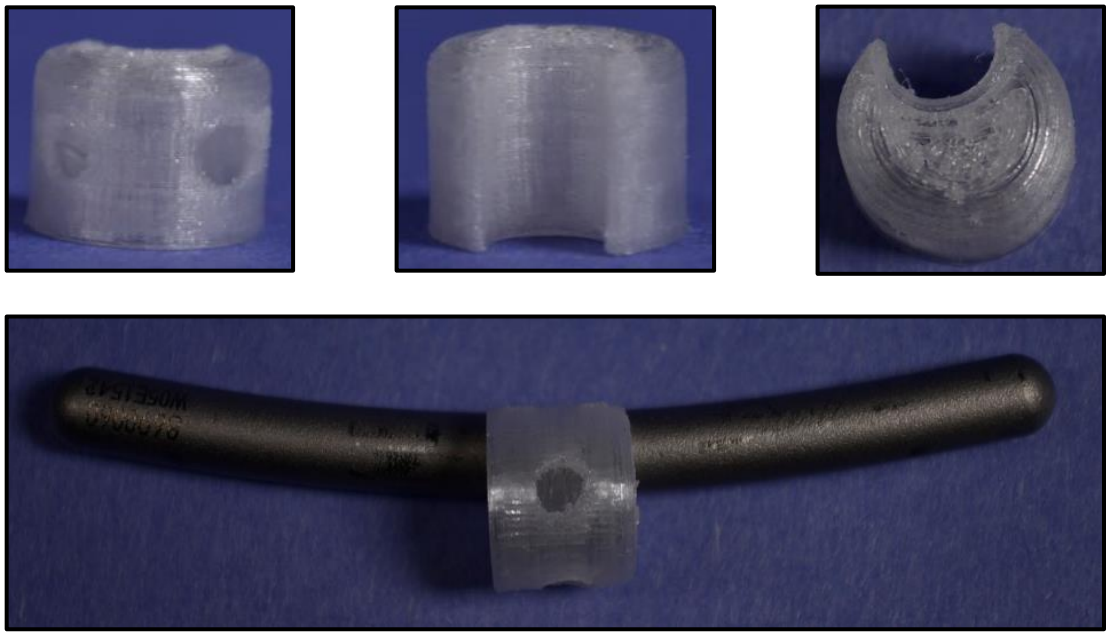

Figure 16: Images of the front, back, top, and the final version of the manufactured clip attached to a spinal fusion rod.

4.5 MicroCT Dimensional Analysis

Three clips were imaged with X-ray microtomography (Scanco, Brüttisellen, Switzerland). The clips were scanned at a resolution of 20 μm. These scans were analyzed for dimensional accuracy utilizing rendering software (Analyze 11.0). Dimensions of interest were the following: height, width, thickness, clip diameter, channel diameter, and channel offset (figure 17).

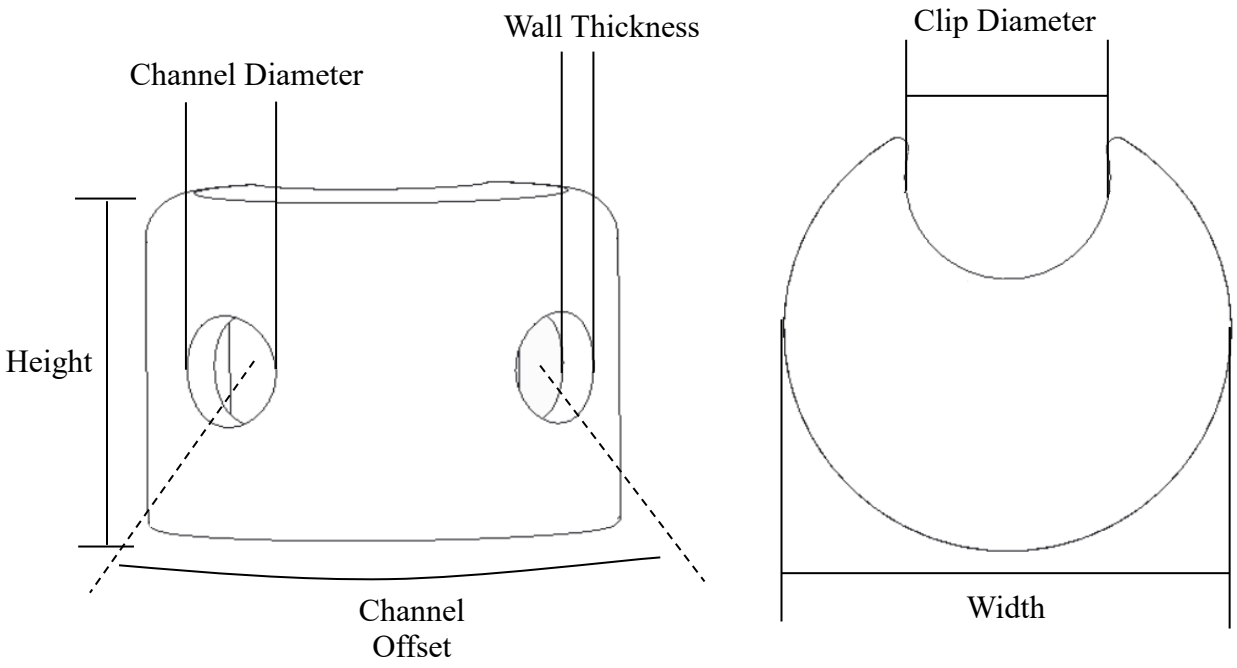

Figure 17: Front (left) and top (right) view of Solidworks drawings of the clip, demonstrating the dimensions measured via μCT imaging.

4.6 Degradation Analysis

Twelve clips, filament, and raw pellets were prepared for degradation analysis. The degradation protocol was prepared in compliance with ASTM F1635 – 16. The samples were individually weighed and placed into phosphate buffer solution (PBS). The samples were kept at a temperature of 37°C, and pH of 7.4 to simulate *in vivo* conditions. Three samples of clips, filament, and raw pellets were removed from the PBS at a time point of one week for the duration of a month. Once removed, the clips were dried with a desiccator and weighed. Mass loss of the clips was evaluated.

4.7 Results

MicroCT dimensional analysis of the printed clips found the clips to be similar to the intended design concerning the height, width, clip diameter, channel diameter, and channel offset. There was a significant difference concerning the wall thickness of the clip ($p = 0.029$; figure 18).

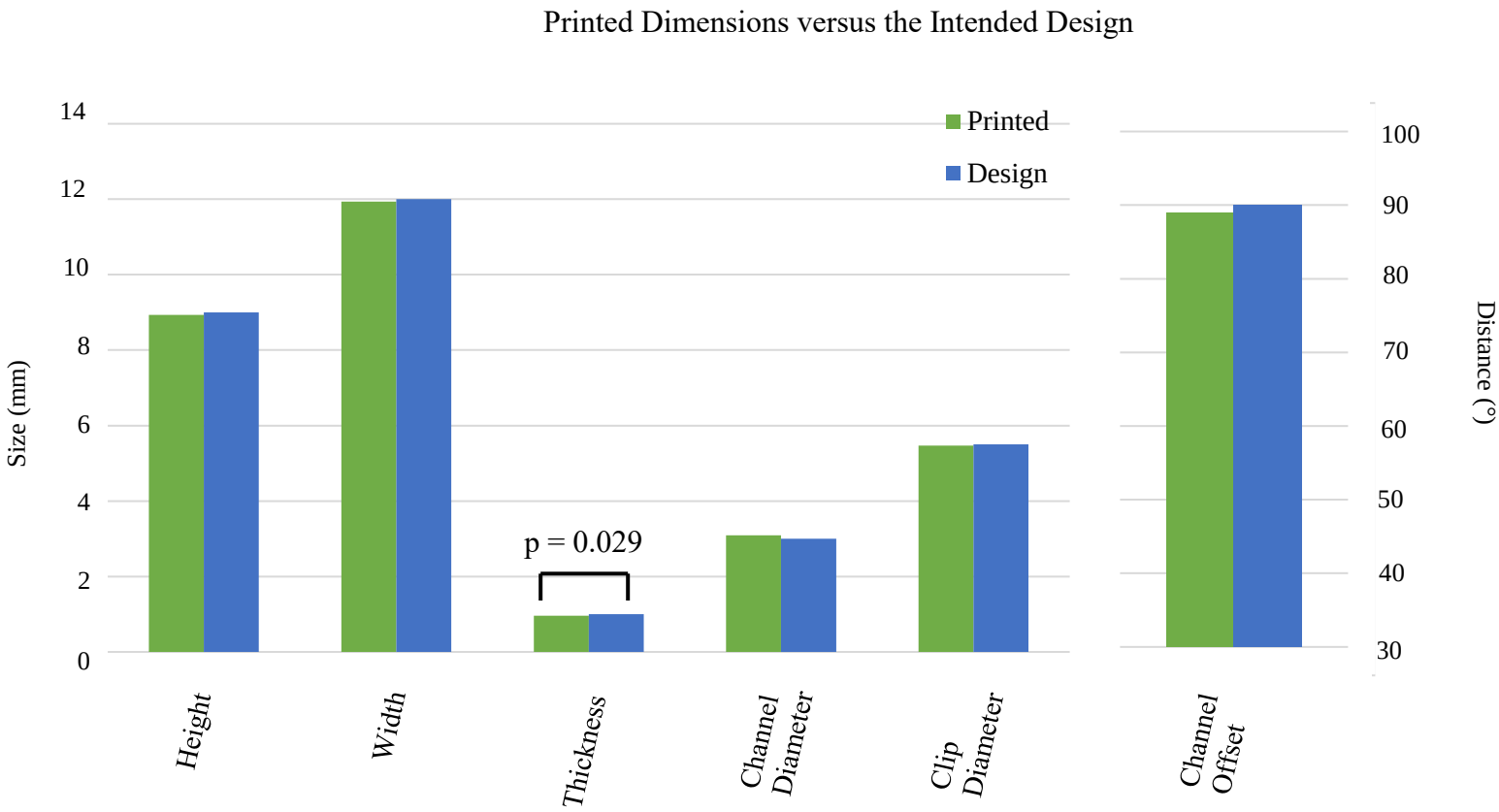

Figure 18: Printed clip dimensions measured with µCT. The measured dimensions were compared the intended dimensions.

The degradation analysis of the raw pellets, filament, and clips found to the rate of degradation to be similar among all three forms of PLDLLA for the first three weeks of degradation; the raw pellets were found to have a significantly slower rate at the fourth week ($p = 0.039$; table 3). The raw pellets, filament, and clips had an average mass loss of 1.8E-3g, 4.1E-3g, and 5.5E-3g over the period of a month, respectively (figure 19).

Table 3: In vitro degradation of clip, filament, and raw pellet samples. Degradation spanned one month and is reported as mass loss (g).

Material Form	Week 1 (g)	Week 2 (g)	Week 3 (g)	Week 4 (g)
Clip	1.0E-4 ± 8.2E-5	9.7E-4 ± 3.1E-4	1.9E-3 ± 1.1E-3	5.5E-3 ± 1.2E-3
Filament	8.0E-4 ± 2.9E-4	9.0E-4 ± 6.7E-4	3.4E-3 ± 6.5E-4	4.1E-3 ± 7.6E-4
Raw pellet	3.3E-5 ± 1.2E-5	4.0E-4 ± 1.6E-4	1.6E-3 ± 7.6E-4	1.8E-3 ± 1.7E-4
P value	0.061	0.190	0.113	0.039

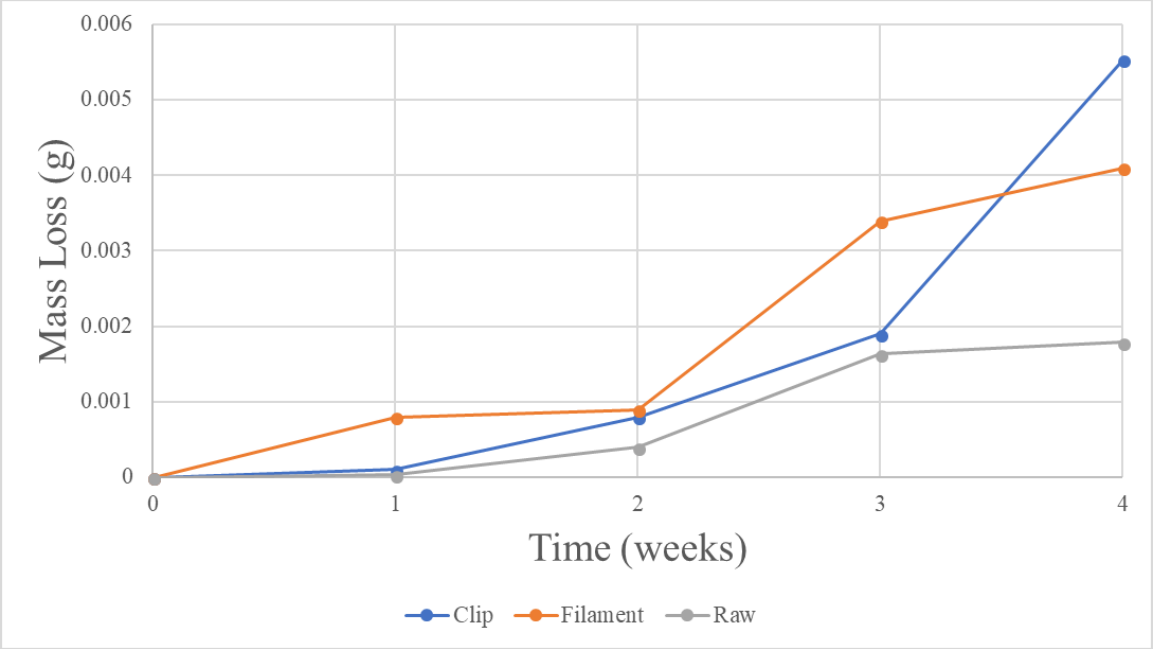

Figure 19: In vitro degradation analysis of clip, filament, and raw pellet samples. Degradation is reported as a mass loss over time.

4.8 Discussion

The fabrication and subsequent analysis of the clips supported both hypotheses. The first hypothesis was confirmed as the clips were able to be printed to dimensions similar to those of the intended design, with the exception of the wall thickness. This difference could be a result of multiple factors. For one, the printer resolution varies from printer to printer and is an indication of print accuracy capabilities. Resolution is the number of voxels that can be placed in a unit volume [34]. This is one of the pitfalls of FFF printers as comparted to other methods of rapid prototyping, such as laser printers, which provide a higher-level accuracy. The resolution of the typical FFF printer is 100 – 300 µm with a tolerance of 200 – 400 µm whereas the typical resolution of a selective laser sinter (SLS) printer is 60 – 150 µm with a tolerance of 50 – 150 µm [70].

Additionally, the diameter of the nozzle may play a role. Specifically, the nozzle utilized here had a 0.4mm diameter. The thickness of the clip was 1 mm which is not an even multiple of the nozzle diameter, possibly decreasing the possible accuracy. Regardless of the cause of the difference it should be noted that the discrepancy was exceedingly small with the difference between the two being 0.0425 ± 0.0109 mm.

The second hypothesis was also supported as the clips only degraded by 0.05% mass after a week of *in vitro* degradation. The various forms of PLDLLA as showed similar degradation rate throughout the first three weeks of degradation however, at week four it was found that the samples degraded at different rate ($p = 0.039$). This difference is likely due to the crystallinity of the raw pellets as seen via DSC analysis. Crystallinity will slow degradation as crystalline regions in a polymer will have stronger secondary bonds, decreasing the amount of water that is able to enter subsequently increasing the time to degradation [36]. Future studies should carry out complete degradation of the all samples to provide a more complete degradation profile.

5. CONCLUSION

5.1 Conclusion

This study demonstrated that the materials applicable to 3D printing are still expanding and have potential in the realm of bioabsorbable polymers. As demonstrated and verified here, bioabsorbable polymers can be taken from pellet form, extruded into filament and utilized for FFF (table 4). However, considerations must be taken should this method progress towards medical application. Although we found the filaments to hold consistent in both molecular weight and thermal properties, the possibility remains that the filament differs in these properties from the raw material. Future work should analyze this potential difference and the implications it may have on the final device. Additionally, we found the manufactured clip to be successful in all but one dimension. This difference is likely due to the size of the nozzle. The clip wall thickness was the smallest dimension and not a multiple of the nozzle diameter. We predict that the difference between the designed and manufactured dimension is a result of this, but further research should be conducted to confirm this. Ultimately, the clip degraded at a rate appropriate for this application despite the impact the processing from raw material to printed clip may have had.

Table 4: Criteria verification methodology utilized in this project.

Requirement No.	Criteria	Verification Method	Results
1	The filament must have consistent thermal properties	DSC Analysis	Thermal properties were consistent
2	The filament must have consistent molecular weight	GPC Analysis	Molecular weight was consistent
3	The clip must have dimensions similar to the intended design	MicroCT Dimensional Analysis	All dimensions were similar except for the wall thickness
4	The clip must not have greater than 1% mass loss after one week of *in vitro* degradation	Degradation Analysis (F1635 – 16)	The clip did not exceed 1% mass loss after one week of *in vitro* degradation.

5.2 Limitations

This study had several limitations. Most importantly, only a one bioabsorbable polymer was evaluated. While it appears that PLDLLA 70/30 is a viable material for this application one must not assume that it is the best option. Other materials should be analyzed in a comparable manner to the study performed here and, if successful, graduate to animal studies. Secondly, mode of production must be evaluated. FFF is rapid and the most cost-effective method of 3D printing however, FFF is not as accurate as other forms of 3D printing, such as SLS. Typical resolutions of FFF printers range from 300µm to 100µm, whereas a typical SLS printer has a resolution of 150µm to 60µm [71]. The

disparity in resolution can have a dramatic impact on print quality. Nevertheless, this increase comes at a much greater cost due to more expensive machinery and material waste. Should this solution to SSI progress, analysis must be performed to determine if the resolution provided by FFF is proficient for this device. Lastly, DSC was determined to have been performed on too small of a sample size, yielding a power of 0.55. Despite these limitations, this study provided evidence that raw pellets of a bioabsorbable polymer can produce a filament of consistent properties to subsequently be utilized for FFF printing.

6. FUTURE WORK

6.1 Characterization

Before proceeding to animal testing the device developed in this thesis should undergo further characterization. Specifically, two variables need to be further addressed. First the device should be imaged with a scanning electron microscope (SEM). A SEM can image the device at a microscopic level enabling the evaluation of the porosity of the device. FFF has been found to be at risk of high porosity due to the cooling of layers between deposition times [72]. This puts the device at risk of absorbing a portion of the antibiotics resulting in a decrease in the amount released at rupture. Additionally, the raw pellets utilized as controls for DSC and GPC analysis may have had different properties than the manufactured filament however, only one sample of raw pellet was analyzed. It may be useful to perform DSC and GPC analysis on a larger sample size to determine if there is a difference and what impact this will have on the final product.

6.2 Mechanical Testing

An individual will undergo flexion of their spine with their daily activities. As a result, the fusion rod will also undergo flexion [73]. This movement has the potential to cause loosening or migration of the clip proposed here. ASTM F1717-01 dictates test methods for spinal implant constructs. Utilizing this standard, cyclic loading should be performed on a spinal rod with attached clip. The construct should undergo five million cycles, simulating two years of moderate activity [74].

6.3 Print Resolution

FFF is the most affordable method of 3D printing. This reduction in cost is accompanied by a decrease in print resolution however, methods have been developed to reduce the difference in print quality. Although the prints produced in this study were similar in all dimensions, with the exception of the wall thickness, improvements can always be made. A potential option for print assistance would be the use of polyvinyl alcohol (PVA). PVA is a water-soluble material used as a support material for FFF printing [75]. PVA adheres well to PLA and has no hazardous by-products when degraded. PVA is available in the form of filament and is very affordable, coming in at a cost of approximately $80/kg. PVA would function as a casing for the PLDLLA clip, providing stability on all print surfaces, and improving printing accuracy. PVA has been reported to dissolve in approximately three hours depending on the volume utilized in conjunction with the print however, no formal study has been conducted to determine the rate when used as a 3D printing support material. As shown by the degradation performed here, the PLDLLA clips had only an 1.6% mass loss over the span of one month. I speculate that PVA would provide a reasonable enhancement to the print accuracy while causing very little to no difference in the clip after dissolution. Further research is required to determine if PVA is a valid option for improvement of print quality or if its required dissolution impacts the PLDLLA clip in an adverse way.

6.4 Coating

The complete design of the device proposed here involves a membrane coating of the device for subsequent rupture of antibiotics. The proposed procedure for the application of the membrane involved dipping the device into liquid PLA and allowing the device to dry for a hard membrane of PLA however, upon testing the membrane of PLA formed was found to be too thick to rupture.

A potential solution is the printing of a PLA coating. Pictured in figure 20 is a 0.15 mm thick sample of PLA printed via FFF. This sample can be adhered to the clip with a small amount of liquid PLA. Testing should be performed to determine if a membrane produced via this method can be ruptured.

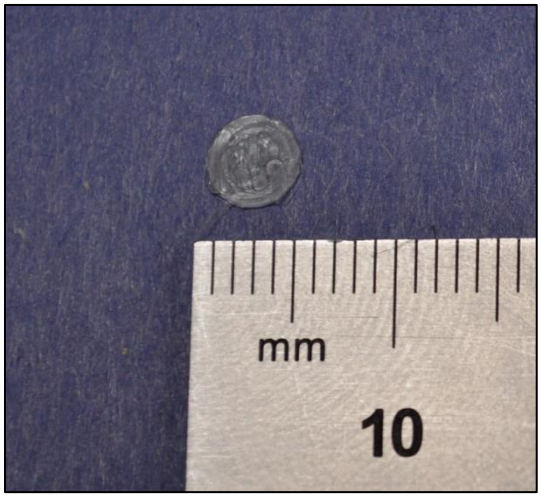

Figure 20: Proposed solution for coating the clip channels from which antibiotics will be dispelled. The PLA print here is 3 mm in diameter and approximately 0.15 mm thick.

6.5 Sterilization

Future testing and development of this device will require implantation of the device. Proper sterilization of the device is required to create a product with potential to be used *in vivo*. Depending on the sterilization process, the properties of the device may be significantly impacted. Three potential sterilization processes are gamma irradiation, electron beam (e-beam) irradiation, and chemical sterilization performed with gases, such as ethylene oxide (EtO) [36]. Gamma irradiation utilizes Cobalt 60 radiation to kill microorganisms and is often used for medical devices, packaging, and pharmaceuticals [76]. E-beam irradiation utilizes high-energy electrons targeted at the device. This results in the DNA double helix of any microorganism on the device being broken, resulting in sterilization of the device [71]. EtO sterilization is often used for medical devices. By placing the device in EtO, the DNA of any microorganism on the device is disrupted, effectively sterilizing the device [72].

Regardless of the method used to sterilize the device, testing must be carried out to determine how the material will respond to said sterilization. Often, sterilization will impact the properties of the material, for example, gamma radiation and e-beam sterilization cause chain scission leading to a decrease in molecular weight [36, 77]. EtO has a similar effect as e-beam, although less dramatically, however EtO carries the risk that harmful levels of the chemical could be left on the surface of the device [78, 79].

Plasma sterilization provides a practical alternative. Low-temperature, low-pressure plasma sterilization has proved to cause no significant impact on molecular weight with concern to 95/5 PLDLLA [79]. Nevertheless, plasma sterilization must be

performed with 70/30 PLDLLA and has its own pitfalls as it can cause micro-etching on the surface of the device [79].

7. **REFERENCES**

[1] Y. C. Lee, M. G. T. Zotti, and O. L. Osti, "Operative Management of Lumbar Degenerative Disc Disease," *Asian spine journal,* vol. 10, no. 4, p. 801, 2016.

[2] J. S. A. Joseph, J. F. Brandoff, M. Menkowitz, J. O'Shea, and M. G. Neuwirth, "Lumbar Spine Fusion: Types, Principles, and Outcomes," *Neurosurgery Quarterly,* vol. 18, no. 1, pp. 34-44, 2008.

[3] C. M. Bono and C. K. Lee, "Critical analysis of trends in fusion for degenerative disc disease over the past 20 years: influence of technique on fusion rate and clinical outcome," *Spine,* vol. 29, no. 4, pp. 455-463, 2004.

[4] W. Davis *et al.*, "Modern spinal instrumentation. Part 1: Normal spinal implants," *Clinical Radiology,* vol. 68, no. 1, pp. 64-74, 2012.

[5] R. D. Peek and L. L. Wiltse, "History of spinal fusion," in *Spinal Fusion*: Springer, 1990, pp. 3-8.

[6] R. C. Mulholland, "Cages: outcome and complications," *European Spine Journal,* vol. 9, no. S1, pp. S110-S113, 2000.

[7] B. M. Ozgur, K. Yoo, G. Rodriguez, and W. R. Taylor, "Minimally-invasive technique for transforaminal lumbar interbody fusion (TLIF)," *European Spine Journal,* vol. 14, no. 9, pp. 887-894, 2005.

[8] I. Guwahati. (2016). *Thermogravimetric Analysis*.

[9] K. E. M. D. Radcliff *et al.*, "What is new in the diagnosis and prevention of spine surgical site infections," *Spine Journal, The,* vol. 15, no. 2, pp. 336-347, 2015.

[10] K. Maruo and S. H. Berven, "Outcome and treatment of postoperative spine surgical site infections: predictors of treatment success and failure," *Journal of Orthopaedic Science,* vol. 19, no. 3, pp. 398-404, 2014.

[11] S. M. Kurtz *et al.*, "Infection risk for primary and revision instrumented lumbar spine fusion in the Medicare population," *Journal of Neurosurgery: Spine,* vol. 17, no. 4, pp. 342-347, 2012.

[12] M. Ishii *et al.*, "Postoperative deep surgical-site infection after instrumented spinal surgery: a multicenter study," *Global spine journal,* vol. 3, no. 2, pp. 95-101, 2013.

[13] O. Royal College of, Gynaecologists, W. s. National Collaborating Centre for, H. Children's, H. National Institute for, and E. Clinical, *Surgical site infection: prevention and treatment of surgical site infection* (no. Book, Whole). London: RCOG Press, 2008.

[14] R. M. Donlan, "Biofilm Formation: A Clinically Relevant Microbiological Process," *Clinical Infectious Diseases,* vol. 33, no. 8, pp. 1387-1392, 2001.

[15] R. O. Darouiche, A. Dhir, A. J. Miller, G. C. Landon, I. I. Raad, and D. M. Musher, "Vancomycin penetration into biofilm covering infected prostheses and effect on bacteria," *Journal of Infectious Diseases,* vol. 170, no. 3, pp. 720-723, 1994.

[16] V. Goz, A. Rane, A. M. Abtahi, B. D. Lawrence, D. S. Brodke, and W. R. Spiker, "Geographic Variations in the Cost of Spine Surgery," *Spine,* vol. 40, no. 17, pp. 1380-1389, 2015.

[17] P. I. J. M. Wuisman and T. M. Smit, *Degradable polymers for skeletal implants* (no. Book, Whole). New York: Nova Science Publishers, 2009.

[18] R. W. Bucholz, S. Henry, and B. M. Henley, "Fixation with bioabsorbable screws for the treatment of fractures of the ankle," *JBJS,* vol. 76, no. 3, pp. 319-324, 1994.

[19] J. E. Bergsma, W. C. de Bruijn, F. R. Rozema, R. R. M. Bos, and G. Boering, "Late degradation tissue response to poly(l-lactide) bone plates and screws," *Biomaterials,* vol. 16, no. 1, pp. 25-31, 1995.

[20] C. Lam, R. Olkowski, W. Swieszkowski, K. Tan, I. Gibson, and D. Hutmacher, "Composite PLDLLA/TCP scaffolds for bone engineering: mechanical and in vitro

evaluations," in *13th International Conference on Biomedical Engineering*, 2009, pp. 1480-1483: Springer.

[21] J. L. Dávila, M. S. Freitas, P. Inforçatti Neto, Z. C. Silveira, J. V. L. Silva, and M. A. d'Ávila, "Fabrication of PCL/β-TCP scaffolds by 3D mini-screw extrusion printing," *Journal of Applied Polymer Science*, vol. 133, no. 15, pp. n/a-n/a, 2016.

[22] M. A. Woodruff and D. W. Hutmacher, "The return of a forgotten polymer—Polycaprolactone in the 21st century," *Progress in Polymer Science*, vol. 35, no. 10, pp. 1217-1256, 2010.

[23] D. Williams, *The Williams Dictionary of Biomaterials* (no. Book, Whole). Liverpool: Liverpool University Press, 1988.

[24] Y. Liu, Y. Zheng, and B. Hayes, "Degradable, absorbable or resorbable—what is the best grammatical modifier for an implant that is eventually absorbed by the body?," *Science China Materials*, vol. 60, no. 5, pp. 377-391, 2017.

[25] B. C. Gross, J. L. Erkal, S. Y. Lockwood, C. Chen, and D. M. Spence, "Evaluation of 3D printing and its potential impact on biotechnology and the chemical sciences," ed: ACS Publications, 2014.

[26] C. W. Hull, "Apparatus for production of three-dimensional objects by stereolithography," ed: Google Patents, 1986.

[27] S. S. Crump, "Apparatus and method for creating three-dimensional objects," ed: Google Patents, 1992.

[28] A. Waldbaur, H. Rapp, K. Laenge, and B. E. Rapp, "Let there be chip—towards rapid prototyping of microfluidic devices: one-step manufacturing processes," *Analytical Methods*, vol. 3, no. 12, pp. 2681-2716, 2011.

[29] D. T. Pham and R. S. Gault, "A comparison of rapid prototyping technologies," *International Journal of machine tools and manufacture*, vol. 38, no. 10-11, pp. 1257-1287, 1998.

[30] K. S. Boparai, R. Singh, and H. Singh, "Development of rapid tooling using fused deposition modeling: a review," *Rapid Prototyping Journal*, vol. 22, no. 2, pp. 281-299, 2016.

[31] W. Zhong, F. Li, Z. Zhang, L. Song, and Z. Li, "Short fiber reinforced composites for fused deposition modeling," *Materials Science and Engineering: A*, vol. 301, no. 2, pp. 125-130, 2001.

[32] M. A. Jafari, W. Han, F. Mohammadi, A. Safari, S. C. Danforth, and N. Langrana, "A novel system for fused deposition of advanced multiple ceramics," *Rapid Prototyping Journal*, vol. 6, no. 3, pp. 161-175, 2000.

[33] C. M. Boutry, R. Kiran, F. Umbrecht, and C. Hierold, "Processing and quantitative analysis of biodegradable polymers (PLLA and PCL) thermal bonding," *Journal of Micromechanics and Microengineering*, vol. 20, p. 085006, 2010.

[34] I. Onyeako, "Resolution-Aware Slicing of CAD Data for 3D Printing," Université d'Ottawa/University of Ottawa, 2016.

[35] O. Topçu, Y. Taşcıoğlu, and H. Ünver, "A method for slicing CAD models in binary STL format," in *6th International Advanced Technologies Symposium (IATS'11)*, 2011, vol. 163, pp. 141-145.

[36] P. Wuisman and T. Smit, "Bioresorbable polymers: heading for a new generation of spinal cages," *European spine journal*, vol. 15, no. 2, pp. 133-148, 2006.

[37] V. Singh and M. Tiwari, "Structure-Processing-Property Relationship of Poly(Glycolic Acid) for Drug Delivery Systems 1: Synthesis and Catalysis," *International Journal of Polymer Science*, vol. 2010, pp. 1-23, 2010.

[38] M. Labet and W. Thielemans, "Synthesis of polycaprolactone: a review," *Chemical Society Reviews*, vol. 38, no. 12, pp. 3484-3504, 2009.

[39] K. Fukushima, C. Abbate, D. Tabuani, M. Gennari, P. Rizzarelli, and G. Camino, "Biodegradation trend of poly(ε-caprolactone) and nanocomposites," *Materials Science & Engineering C,* vol. 30, no. 4, pp. 566-574, 2010.

[40] S. Holland and B. Tighe, "Biodegradable polymers," *Advances in pharmaceutical science,* vol. 6, pp. 101-164, 1992.

[41] P. A. Gunatillake and R. Adhikari, "Biodegradable synthetic polymers for tissue engineering," *Eur Cell Mater,* vol. 5, no. 1, pp. 1-16, 2003.

[42] C. C. Rusa and A. E. Tonelli, "Polymer/polymer inclusion compounds as a novel approach to obtaining a PLLA/PCL intimately compatible blend," *Macromolecules,* vol. 33, no. 15, pp. 5321-5324, 2000.

[43] J. G. Lyons, P. Blackie, and C. L. Higginbotham, "The significance of variation in extrusion speeds and temperatures on a PEO/PCL blend based matrix for oral drug delivery," *International journal of pharmaceutics,* vol. 351, no. 1-2, pp. 201-208, 2008.

[44] R. M. Aghdam, S. Najarian, S. Shakhesi, S. Khanlari, K. Shaabani, and S. Sharifi, "Investigating the effect of PGA on physical and mechanical properties of electrospun PCL/PGA blend nanofibers," *Journal of Applied Polymer Science,* vol. 124, no. 1, pp. 123-131, 2012.

[45] M. Spoerk, J. Gonzalez-Gutierrez, J. Sapkota, S. Schuschnigg, and C. Holzer, "Effect of the printing bed temperature on the adhesion of parts produced by fused filament fabrication," *Plastics, Rubber and Composites,* vol. 47, no. 1, pp. 17-24, 2018.

[46] D. Garlotta, "A literature review of poly (lactic acid)," *Journal of Polymers and the Environment,* vol. 9, no. 2, pp. 63-84, 2001.

[47] H. Dardik, I. Dardik, and H. Laufman, "Clinical use of polyglycolic acid polymer as a new absorbable synthetic suture," *The American Journal of Surgery,* vol. 121, no. 6, pp. 656-660, 1971.

[48] J. Braunecker, M. Baba, G. E. Milroy, and R. E. Cameron, "The effects of molecular weight and porosity on the degradation and drug release from polyglycolide," *International Journal of Pharmaceutics,* vol. 282, no. 1, pp. 19-34, 2004.

[49] A. Weiler, H.-J. Helling, U. Kirch, T. K. Zirbes, and K. E. Rehm, "Foreign-body reaction and the course of osteolysis after polyglycolide implants for fracture fixation: experimental study in sheep," *Bone & Joint Journal,* vol. 78, no. 3, pp. 369-376, 1996.

[50] M. H. Kudur, S. B. Pai, H. Sripathi, and S. Prabhu, "Sutures and suturing techniques in skin closure," *Indian Journal of Dermatology, Venereology and Leprology,* vol. 75, no. 4, pp. 425-434, 2009.

[51] A. Pandey, G. C. Pandey, and P. B. Aswath, "Synthesis of polylactic acid–polyglycolic acid blends using microwave radiation," *Journal of the mechanical behavior of biomedical materials,* vol. 1, no. 3, pp. 227-233, 2008.

[52] A. R. Vaccaro *et al.*, "The use of bioabsorbable implants in the spine," vol. 3, ed. United States: Elsevier Inc, 2003, pp. 227-237.

[53] O. Böstman and H. Pihlajamäki, "Clinical biocompatibility of biodegradable orthopaedic implants for internal fixation: a review," *Biomaterials,* vol. 21, no. 24, pp. 2615-2621, 2000.

[54] J. O. Hollinger and G. C. Battistone, "Biodegradable bone repair materials: synthetic polymers and ceramics," ARMY INST OF DENTAL RESEARCH WASHINGTON DC1985.

[55] J. M. Toth *et al.*, "Evaluation of 70/30 poly (L-lactide-co-D,L-lactide) for use as a resorbable interbody fusion cage," *Journal of neurosurgery,* vol. 97, no. 4 Suppl, p. 423, 2002.

[56] D. E. Chang, H. C. Jung, J. S. Rhee, and J. G. Pan, "Homofermentative production of D- or L-lactate in metabolically engineered Escherichia coli RR1," *Applied and environmental microbiology,* vol. 65, no. 4, pp. 1384-1389, 1999.

[57] A. U. Daniels, M. K. Chang, and K. P. Andriano, "Mechanical properties of biodegradable polymers and composites proposed for internal fixation of bone," vol. 1, ed. UNITED STATES, 1990, pp. 57-78.

[58] M. Therin, P. Christel, S. Li, H. Garreau, and M. Vert, "In vivo degradation of massive poly(α-hydroxy acids): Validation of In vitro findings," *Biomaterials,* vol. 13, no. 9, pp. 594-600, 1992.

[59] G. G. Pitt, M. M. Gratzl, G. L. Kimmel, J. Surles, and A. Sohindler, "Aliphatic polyesters II. The degradation of poly (DL-lactide), poly (ε-caprolactone), and their copolymers in vivo," *Biomaterials,* vol. 2, no. 4, pp. 215-220, 1981.

[60] M. van Dijk, T. H. Smit, M. F. Arnoe, E. H. Burger, and P. I. J. M. Wuisman, "The use of poly-L-lactic acid in lumbar interbody cages - design and biomechanical evaluation in vitro," *European Spine Journal,* vol. 12, no. 1, pp. 34-40, 2003.

[61] O. M. Böstman and H. K. Pihlajamäki, "Adverse tissue reactions to bioabsorbable fixation devices," *Clinical orthopaedics and related research,* vol. 371, pp. 216-227, 2000.

[62] G. Maglio, A. Migliozzi, R. Palumbo, B. Immirzi, and M. G. Volpe, "Compatibilized poly (ϵ-caprolactone)/poly (l-lactide) blends for biomedical uses," *Macromolecular rapid communications,* vol. 20, no. 4, pp. 236-238, 1999.

[63] W.-C. Lai, W.-B. Liau, and T.-T. Lin, "The effect of end groups of PEG on the crystallization behaviors of binary crystalline polymer blends PEG/PLLA," *Polymer,* vol. 45, no. 9, pp. 3073-3080, 2004.

[64] T. H. Smit, M. R. Krijnen, M. van Dijk, and P. I. J. M. Wuisman, "Application of polylactides in spinal cages: Studies in a goat model," *Journal of Materials Science: Materials in Medicine,* vol. 17, no. 12, pp. 1237-1244, 2006.

[65] A. Frost, E. Bagouri, M. Brown, and V. Jasani, "Osteolysis following resorbable poly-l-lactide-co-d, l-lactide PLIF cage use: a review of cases," *European Spine Journal*, vol. 21, no. 3, pp. 449-454, 2012.

[66] P. Johnathan Stolk, "TA INSTRUMENTS DIFFERENTIAL SCANNING CALORIMETER (DSC) ".

[67] M. J. O'Neill, "The Analysis of a Temperature-Controlled Scanning Calorimeter," *Analytical Chemistry*, vol. 36, no. 7, pp. 1238-1245, 1964.

[68] P. S. L. Center. *Glass Transition*. Available: http://pslc.ws/macrog/tg.htm

[69] C. Migliaresi, A. De Lollis, L. Fambri, and D. Cohn, "The effect of thermal history on the crystallinity of different molecular weight PLLA biodegradable polymers," *Clinical Materials*, vol. 8, no. 1, pp. 111-118, 1991.

[70] A. Rae, "Prototyping Overview," 2006.

[71] formlabs, "The Ultimate Guide to Stereolithography (SLA) 3D Printing," 2017.

[72] K. J. Christiyan, U. Chandrasekhar, and K. Venkateswarlu, "A study on the influence of process parameters on the Mechanical Properties of 3D printed ABS composite," in *IOP Conference Series: Materials Science and Engineering*, 2016, vol. 114, no. 1, p. 012109: IOP Publishing.

[73] C. Lindsey, V. Deviren, Z. Xu, R. F. Yeh, and C. M. Puttlitz, "The effects of rod contouring on spinal construct fatigue strength," *SPINE*, vol. 31, no. 15, pp. 1680-1687, 2006.

[74] *Standard Test Methods for Spinal Implant Constructs in a Vertebrectomy Model*, F1717-01, 2002.

[75] (2017). *Technical Data Sheet PVA*.

[76] M. Coimbra, C. Elias, and P. Coelho, "In vitro degradation of poly-L-D-lactic acid (PLDLA) pellets and powder used as synthetic alloplasts for bone grafting," *Journal of Materials Science: Materials in Medicine,* vol. 19, no. 10, pp. 3227-3234, 2008.

[77] M. Mansouri, A. Berrayah, C. Beyens, C. Rosenauer, C. Jama, and U. Maschke, "Effects of electron beam irradiation on thermal and mechanical properties of poly(lactic acid) films," *Polymer Degradation and Stability,* vol. 133, pp. 293-302, 2016.

[78] I. Matthews, C. Gibson, and A. Samuel, "Enhancement of the kinetics of the aeration of ethylene oxide sterilized polymers using microwave radiation," *Journal of Biomedical Materials Research Part A,* vol. 23, no. 2, pp. 143-156, 1989.

[79] S. Gogolewski, P. Mainil-Varlet, and J. Dillon, "Sterility, mechanical properties, and molecular stability of polylactide internal-fixation devices treated with low-temperature plasmas," *Journal of Biomedical Materials Research Part A*, vol. 32, no. 2, pp. 227-235, 1996.